Evaluation of Tinnitus and Hearing Loss in the Adult

15

Graham C. Keir, Jenny K. Hoang, and C. Douglas Phillips

Abstract

Tinnitus and hearing loss in the adult can have profound effects on quality of life. The imaging workup for tinnitus and hearing loss in adults follows otoscopic exam and audiometry testing. CT and MR imaging have different and often complimentary roles in the evaluation of tinnitus and hearing loss, depending on the clinical scenario and the suspected underlying etiology. Imaging can often identify the cause and evaluate the extent of disease for surgical planning. This article discusses anatomy, imaging techniques, and pathologies that cause tinnitus and hearing loss with a mass and without a mass.

Keywords

Temporal bone · Hearing loss · Tinnitus · Otospongiosis
Labyrinthitis ossificans · Superior semicircular canal dehiscence · Enlarged vestibular aqueduct syndrome
Vestibular schwannoma

Learning Objectives

- Identify key anatomical structures in the temporal bone.
- Describe the role of CT and MRI for temporal bone imaging.
- Differentiate between diseases of the temporal bone on imaging and describe their clinical presentation.

Key Points

- Imaging can identify the cause and evaluate the extent of disease for surgical planning.
- The common causes of tinnitus and hearing loss without a mass include otospongiosis, labyrinthitis ossificans, superior semicircular canal dehiscence, and enlarged vestibular aqueduct syndrome.
- Otospongiosis affects the bony labyrinth while labyrinthitis ossificans affects the membranous labyrinth.
- Vestibular schwannomas often present with non-pulsatile tinnitus and high frequency sensorineural hearing loss.

15.1 Introduction

Tinnitus and hearing loss in the adult can have profound effects on quality of life. Tinnitus is relatively common, with an estimated prevalence of 10–15%, severely impairing approximately 1–2% of all people [1]. Tinnitus is the perception of sound when no external sound is present and may be described as ringing, buzzing, swishing, or clicking sensations. Hearing loss is also common, causing disability in approximately 5% of the world population is indeed "common" and it is indeed referred to as one of the most common disabilities [2]. Hearing loss has several diverse causes and ranges from a partial to total inability to hear sounds. Hearing loss and tinnitus can occur concurrently or in isolation. The role of imaging is to help identify the etiology of these symptoms and evaluate the extent of disease.

G. C. Keir · C. D. Phillips (✉)
Weill Cornell Medical College, NewYork-Presbyterian Hospital, New York, NY, USA
e-mail: qgk9003@nyp.org; cdp2001@med.cornell.edu

J. K. Hoang
Johns Hopkins School of Medicine, Baltimore, MD, USA

J. Hodler et al. (eds.), *Diseases of the Brain, Head and Neck, Spine 2024-2027*, IDKD Springer Series,
https://doi.org/10.1007/978-3-031-50675-8_15

15.2 Causes of Tinnitus and Hearing Loss

15.2.1 Tinnitus

Tinnitus may be categorized as (1) pulsatile or non-pulsatile, (2) primary (idiopathic) or secondary (due to another condition), and (3) subjective or objective. Evaluation of tinnitus begins with otoscopic examination to evaluate for a vascular retro-tympanic mass, audiometric examination, and a review of the patient's medical history and medications. This evaluation helps to determine if imaging is necessary and if so, what study or studies are indicated.

15.2.1.1 Pulsatile Tinnitus

Causes include vascular masses (glomus tympanicum), aberrant arterial or venous anatomy, vascular malformations, and intracranial hypertension. Objective tinnitus (auscultation of a bruit on physical examination) is uncommon and has been attributed to turbulent flow in the setting of dural fistulas, atherosclerotic carotid artery disease, jugular bulb abnormalities, and large condylar or mastoid emissary veins.

15.2.1.2 Non-pulsatile Tinnitus

Causes include cerumen impaction, middle ear infection, mass, medications, noise-induced hearing loss, presbycusis or chronic bilateral hearing loss, hemorrhage, neurodegeneration, and spontaneous intracranial hypotension.

15.2.2 Hearing Loss

Clinical assessment and audiometric testing can determine the type of hearing loss as conductive, sensorineural, or mixed and guide subsequent diagnostic imaging. Conductive hearing loss results from diseases affecting the conduction of mechanical sound wave energy to the cochlea. Sensorineural hearing loss is caused by diseases that impair the cochlear function or the transmission of electrical signal along the auditory pathway.

15.2.2.1 Conductive Hearing Loss

Causes include otospongiosis (commonly a mixed conductive/sensorineural loss), ossicular erosion or fusion, round window occlusion, dehiscence of the superior semicircular canal, and cholesteatoma or neoplasm with suspected intracranial or inner ear extension.

15.2.2.2 Sensorineural Hearing Loss

Causes include labyrinthine ossificans, vestibular schwannoma, and fractures extending across the otic capsule.

15.3 Anatomy

The temporal bone is comprised of five parts: the petrous, tympanic, mastoid, styloid, and squamous segments. The petrous, tympanic, and mastoid segments form the external auditory canal, middle ear, inner ear, and internal auditory canal. These are the most relevant areas to review for hearing loss and tinnitus.

15.3.1 External Auditory Canal

The external auditory canal (EAC) extends from the auricle to the tympanic membrane. The lateral one third of the EAC is fibrocartilaginous, while the medial two-thirds are surrounded by the tympanic portion of the temporal bone.

15.3.2 Middle Ear

The middle ear cavity contains the ossicular chain which conducts sound from the tympanic membrane laterally, to the oval window and inner ear structures medially. The roof of the middle ear is the tegmen tympani and the jugular wall is the floor. The middle ear can be subdivided into the epitympanum (attic) superior to the level of the tympanic membrane, mesotympanum at the level of tympanic membrane, and hypotympanum inferior to the level of tympanic membrane. The epitympanum communicates with the mastoid via the aditus ad antrum.

The mesotympanum contains the majority of the ossicular chain. The ossicular chain is composed of three bones: the malleus, incus, and stapes. Since the stapes is anchored to the oval window, a mnemonic for the order of the ossicles is "MISO" representing *M*alleus, *I*ncus, *S*tapes, and *O*val window. The manubrium of the malleus is attached to the tympanic membrane, and the head of the malleus articulates with the body of the incus in the epitympanum forming the incudomalleolar joint, which has a characteristic "ice cream cone" configuration on axial sections. The lenticular process of the incus extends at approximately a right angle from the long process of the incus to articulate with the capitulum (head) of the stapes, forming the incudostapedial joint.

An important middle ear structure is the scutum, an angular bony projection to which the tympanic membrane attaches superiorly. Prussak space or the lateral epitympanic space, the location for pars flaccida cholesteatomas, is bounded by the scutum laterally and the neck of the malleus medially. The posterior wall of the middle ear is irregular and includes the sinus tympani, pyramidal eminence, and facial recess.

15.3.3 Inner Ear

The inner ear consists of the osseous labyrinth, which includes the cochlea, vestibule, and semicircular canals. The cochlea contains the end organ for hearing while the vestibule and semicircular canals are responsible for balance and equilibrium. The otic capsule surrounds the osseous labyrinth and is considered the densest bone in the human skeleton [3]. The osseous labyrinth encapsulates the membranous labyrinth, which contains endolymph and is separated from the bony walls by perilymph. The endolymph and perilymph do not usually communicate, and there are contrast-enhanced MRI techniques that allow their separate visualization [4].

The cochlea is a spiral-shaped structure with 2½ to 2¾ turns, including the basal, middle, and apical turns, which are separated by interscalar septae. The lateral aspect of the basal turn of the cochlea bulges into the middle ear cavity, forming the cochlear promontory. The nerve of Jacobson (a branch of cranial nerve IX) courses over the cochlear promontory. The cochlear nerve passes from the internal auditory canal through the bony canal for the cochlear nerve (also referred to as the cochlear fossette or cochlear aperture) into the modiolus, a crown-shaped structure centered within the cochlea that transmits branches of the cochlear nerve to the organ of Corti. The organ of Corti is the end organ for hearing and is not visible on CT images.

The bony vestibule is an ovoid space located superior and posterior to the cochlea, which connects to the semicircular canals. There are three semicircular canals—superior, posterior, and lateral, oriented orthogonally to one another. The endolymphatic duct extends from the posterior aspect of the vestibule toward the posterior cranial fossa, ending in a blind pouch, the endolymphatic sac, at the posterior margin of the petrous ridge. The osseous vestibular aqueduct surrounds the endolymphatic duct and normally measures up to 1 mm at the midpoint and 2 mm at the operculum, according to the Cincinnati criteria [5].

The cochlear aqueduct should not be mistaken for a fracture. It is a narrow bony channel that surrounds the perilymphatic duct and extends from the basal turn of the cochlea to the subarachnoid space adjacent to the pars nervosa of the jugular foramen.

15.3.4 Internal Auditory Canal

The internal auditory canal (IAC) is a channel in the petrous bone extending from the fundus, which abuts the labyrinth, to the porus acusticus. At the fundus, a horizontal crest (crista falciformis) divides the IAC into superior and inferior compartments. A vertical crest ("Bill's bar") divides the superior compartment into anterior and posterior components. The facial nerve is in the anterosuperior compartment, the cochlear nerve in the anteroinferior compartment, and the superior and inferior vestibular nerves in the superoposterior and inferoposterior compartments, respectively. A mnemonic for the location of the nerves in the anterior compartment is "Seven (cranial nerve VII) Up, Coke (cochlear nerve) down."

15.4 Imaging Modalities and Techniques

While CT is often the first modality utilized to assess suspected pathology involving the inner ear structures (cochlea and labyrinth), certain lesions such as a cochlear schwannoma and labyrinthine hemorrhage are better detected with MRI. In the workup of subjective pulsatile tinnitus, CT is frequently the preferred modality. However, MR imaging with MRA and MRV may be more appropriate in the workup of objective pulsatile tinnitus (audible bruit on auscultation by the clinician). Conventional catheter angiography may then follow to further characterize the vascular abnormality as well as to provide therapeutic management (embolization) of lesions such as dural fistulas. MR imaging is the primary modality for evaluating the non-osseous components of the temporal bone, suspected retrocochlear pathology, and sensorineural hearing loss. Magnetic resonance imaging is required when temporal bone pathology is suspected to involve the intracranial compartment.

15.4.1 Computed Tomography

15.4.1.1 Temporal Bone CT Technique

Dual acquisition temporal bone CT (separately acquired direct axial and direct coronal images) has been replaced with multi-detector row CT (MDCT) in which a single set/volume of axial images are acquired and reformatted in multiple planes. Thoughtfully performed MDCT reduces radiation dose, and its rapid acquisition minimizes artifact from patient motion. Intravenous contrast is typically not used with temporal bone CT. When contrast is necessary (tumors, vascular pathology such as dural fistulas), higher resolution MRI, MRI with MRA, or CTA are more commonly.

To acquire temporal bone CT, the patient lies supine in the gantry with the head angled superiorly and posteriorly. The neck is hyperextended so that the orbits are canted out of the pathway of the X-ray beam, minimizing exposure to the lens. Gantry tilt may need to be avoided to facilitate image reconstruction and reformats. The scan coverage is from the roof of the temporal bone (the arcuate eminence) through the mastoid tip. A collimation of 0.5–1.0 mm provides appropriate resolution. The raw data from each ear is most often reconstructed into 0.6–0.75 mm thin axial images using an edge-enhancing (bone) algorithm at a DFOV of 70–100 mm

that effectively magnifies the images. Technologists provide reconstructed images including 0.6–1.0 mm reformats in the axial plane parallel to the lateral semicircular canal created from a sagittal plane, and 0.6–1.0 mm reformats in the coronal plane. Axial images with 2–3 mm section thickness of the entire scan volume are also provided in soft tissue algorithm.

Reformats may be obtained in sagittal or oblique planes to improve the detection of pathology in specific clinical settings such as superior semicircular canal dehiscence.

Stenvers reformat: On the console, the technologist scrolls through the sagittal plane until a view of the lateral semicircular canal is obtained. A reformatted axial plane parallel to the lateral semicircular canal is made. The technologist then scrolls through this axial data set and Stenvers reformats are made by tracing a line perpendicular to the long axis of the summit of the superior semicircular canal at submillimetric intervals. This plane is perpendicular to the roof of the superior semicircular canal displaying it in cross section.

Pöschl reformat: On the console, the technologist scrolls through the sagittal plane until a view of the lateral semicircular canal is obtained. A reformatted axial plane parallel to the lateral semicircular canal is made. The technologist then scrolls through this axial data set and Poschl reformats are made by tracing a line parallel to the long axis of the summit of the superior semicircular canal at submillimetric intervals.

15.4.2 Magnetic Resonance Imaging

MRI of the temporal bones is performed in a head coil and should include thin section unenhanced and enhanced axial T1-weighted images, and enhanced coronal T1-weighted images. Fat suppression in at least one enhanced plane may be performed to distinguish fat from enhancement, particularly in the region of the petrous apex. A maximum section thickness of 3 mm with no interslice gap and a small FOV are required to provide images able to depict the fine detail of the anatomy and pathology in the temporal bone. 3D T1-weighted techniques may allow submillimetric scanning on many platforms. 3D T2-weighted techniques are commonly available and valuable in temporal bone imaging to evaluate the relationship of pathologic processes such as a vestibular schwannoma with the surrounding nerves, the patency of labyrinthine structures, the size of the endolymphatic duct and sac, and the extent of cochlear dysplasia in congenital or developmental hearing loss. Reformatted oblique sagittal images perpendicular to the long axis of the internal auditory canal are helpful in identifying cranial nerve hypoplasia or aplasia. Diffusion-weighted imaging (DWI) can help in distinguishing cholesteatoma (restricted diffusion) from inflammatory middle ear cavity opacification (facilitated diffusion). For this purpose, non-echo planar diffusion-weighted imaging outperforms echo-planar imaging as it is less prone to susceptibility artifact and is capable of thin-slice imaging [4, 6].

Axial T2-weighted, T2 FLAIR, and enhanced T1-weighted images of the brain should be performed to assess for intracranial extension of temporal bone pathology. These brain sequences may also exclude central nervous system pathology such as demyelinating disease, stroke, or inflammation/infection that might produce tinnitus, vertigo, hearing loss, or cranial nerve symptoms.

15.5 Tinnitus and Hearing Loss Without a Mass

When no mass is seen on imaging, the radiologist should closely review the inner ear structures. The common causes of tinnitus and hearing loss without a mass include otospongiosis, labyrinthitis ossificans, superior semicircular canal dehiscence, and enlarged vestibular aqueduct syndrome.

15.5.1 Otospongiosis

Otospongiosis (also referred to as otosclerosis) is an idiopathic progressive disease of pathological bone remodeling that causes conductive, sensorineural, or mixed hearing loss. It results in spongiosis or sclerosis of portions of the petrous bone. Conductive hearing loss is usually secondary to abnormal bone encroaching on stapes with impingement on the stapes footplate. Therefore, stapes surgery is the traditional initial treatment for otosclerosis, but is being augmented or replaced by innovations in hearing aid technology and cochlear implants.

Symptoms typically start in the second or third decade of life and presentation is with progressive conductive hearing loss (approximately 80% bilateral [7]) with a normal tympanic membrane, and no evidence of middle ear inflammation. On otoscopic examination, the promontory may have a faint pink tinge reflecting the vascularity of the lesion, referred to as the Schwartze sign.

On imaging, the disease is seen as lucency in the otic capsule. The most common location of involvement of otosclerosis is the bone just anterior to the oval window at a small cleft known as the fissula ante fenestram (*fenestral otosclerosis*) (Fig. 15.1). Involvement of the otic capsule separable from the oval window is referred to as "retrofe-

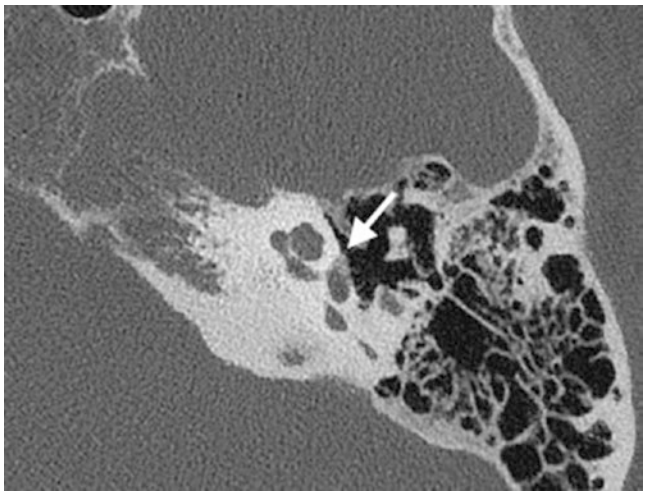

Fig. 15.1 Fenestral otospongiosis on the left with signs of lucency in the fissula ante fenestram (arrow)

nestral otosclerosis" or "cochlear otosclerosis" and can give a sensorineural component to the hearing loss. The Symons and Fanning grading system for otospongiosis has shown to have excellent inter- and intra-observer agreement [7, 8].

A later presumably less active phase can occur where the bone becomes denser and more sclerotic. The bone still appears to encroach on the footplate but has a density closer to that of the otic capsule making it more difficult to identify.

15.5.2 Labyrinthitis Ossificans

Labyrinthitis ossificans is the late stage of labyrinthitis, in which there is pathologic ossification of spaces within the membranous labyrinth. Profound bilateral hearing loss from labyrinthitis ossificans is most commonly due to bacterial meningitis with onset of symptoms 3–4 months after the episode [9]. Other causes include trauma, hemorrhage, autoimmune disease, vascular obstruction of labyrinthine artery, and surgical insult.

Imaging can detect the evolution of labyrinthitis in three stages: acute, fibrous, and ossification. In the acute stage, enhancement of the inner ear is noted on MR images, while the CT images may appear normal. In the intermediate fibrous stage of labyrinthitis, there is loss of fluid signal intensity on heavily T2-weighted sequence images (Fig. 15.2), while the CT scan may still appear normal. In the late ossific stage, there is replacement of the normal cochlea, vestibule, and/or semicircular canals by bone attenuation, now evident on CT [10].

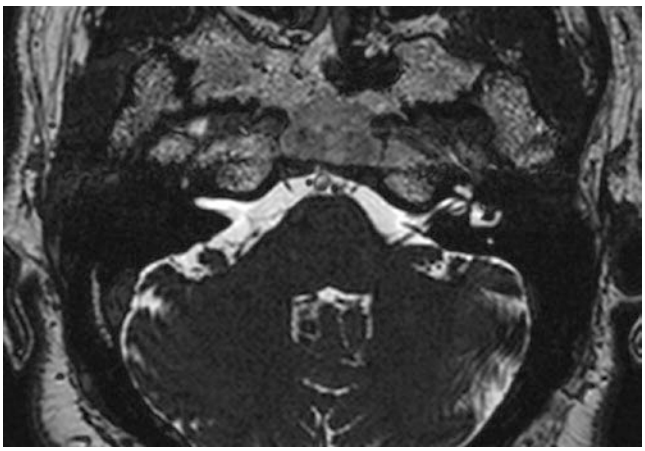

Fig. 15.2 Labyrinthitis ossificans on the right with loss of fluid signal intensity on heavily T2-weighted sequence images

15.5.3 Superior Semicircular Canal Dehiscence

Superior semicircular canal dehiscence is the most common type of third window abnormalities. The labyrinth is normally in a closed hydraulic system with the oval and round windows. Defects in the integrity of the bony structure of the inner ear can decompress/dampen the energy of the sound wave resulting in conductive hearing loss.

In addition to conductive hearing loss, superior semicircular canal dehiscence can present with characteristic symptoms of vertigo when exposed to loud sounds (Tullio phenomenon). This is because of movement of fluid in the superior canal without movement in other canals. Other symptoms include autophony and pulsatile tinnitus. At audiometry, there is a characteristic low-frequency air-bone gap due to decreased air conduction and increased bone conduction.

On imaging, there is a defect in the superior semicircular canal, best seen in the coronal plane, and on reformatted oblique images in the Stenvers plane (perpendicular to the canal). The Pöschl plane shows the superior canal as a ring and helps to determine the length of a dehiscence (Fig. 15.3). The defect is typically along the superior arc of the superior canal along the floor of the middle cranial fossa. However, a defect can also occur along the posterior limb of the canal facing the posterior fossa.

Other third windows abnormalities present with similar symptoms and include enlargement of the opening of the vestibular aqueduct, dehiscence of the scala vestibuli side of the cochlea, erosion of the lateral semicircular canal by cholesteatoma, and abnormal bony thinning between the cochlea and vascular channels. The presence of a defect does not mean that the patient will necessarily have symptoms or will benefit from surgery. Asymptomatic defects are rare (2% of

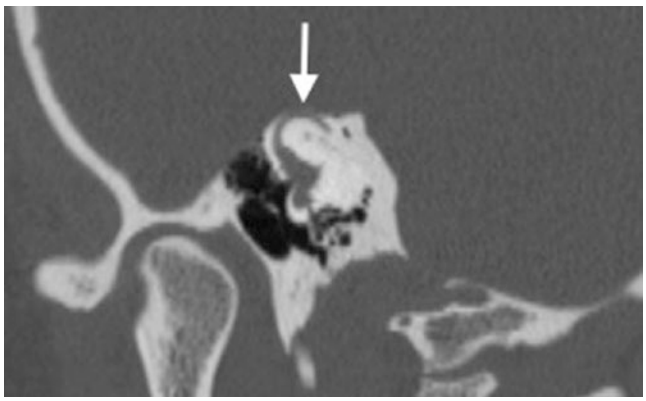

Fig. 15.3 Superior semicircular canal dehiscence on the left. There is a bone defect (arrow) in the superior semicircular canal. Pöschl plane shows the superior canal as a ring and helps to determine the length of a dehiscence

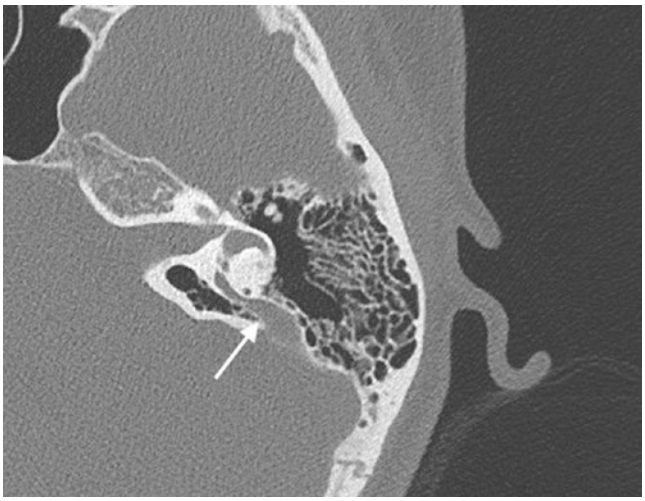

Fig. 15.4 Enlarged vestibular aqueduct. The vestibular aqueduct extends from the posterior aspect of the vestibule toward the posterior cranial fossa (arrow)

the population) so further audiometric evaluation is recommended for all patients with imaging findings [11].

15.5.4 Enlarged Vestibular Aqueduct Syndrome

Most congenital hearing malformations are detected after birth on newborn hearing screening. The exception is enlarged vestibular aqueduct syndrome (EVA) which can progress in childhood or less commonly early adulthood [12]. Stable hearing is observed in 67% of ears with EVA of which 34% will demonstrate fluctuations in hearing. Progression of hearing loss is seen in 33% of ears of which half will demonstrate fluctuations [13].

During fetal development, the vestibular aqueduct starts out as a wide tube. By the fifth week it narrows, and by midterm it approaches adult dimension and shape. However, the vestibular aqueduct continues to grow and change until a child is 3–4 years old. Yet incompletely understood genetic and/or environmental conditions cause EVA.

It is unclear whether EVA actually causes hearing loss, or if instead EVA and hearing loss are caused by the same underlying defect (gene mutation). Supporting this latter theory is the observation that there is an association of EVA with modiolar deficiency [14] as well as the discovery of a specific gene mutation, SLC26A4, which is found in approximately ¼ of patients with EVA [15] and seen in many patients with Pendrad syndrome. Other syndromic causes of EVA include branchio-oto-renal syndrome and CHARGE syndrome.

On clinical exam, hearing loss can be conductive, mixed or sensorineural, and the loss may be stable or fluctuating. Imaging is both diagnostic and prognostic (Fig. 15.4). There are several definitions of an enlarged vestibular aqueduct. The most sensitive criteria are the Cincinnati criteria which defines abnormal as greater than 0.9 mm at the midpoint or greater than 1.9 mm at the operculum in the axial view [5]. Another frequently used criterion is comparison with the semicircular canals—the vestibular aqueduct is considered enlarged if the width of the proximal intraosseous portion exceeds that of the adjacent posterior semicircular canal. A retrospective study has found the severity of hearing loss in patients with an EVA is influenced by degree of widening of the vestibular aqueduct midpoint width [16].

15.6 Tinnitus and Hearing Loss with a Mass

15.6.1 Vestibular Schwannoma

Vestibular schwannomas typically arise from perineural Schwann cells of the superior or inferior vestibular nerve in the internal auditory canal, near the porus acusticus. They may extend into the cerebello-pontine angle. Vestibular schwannomas often present with non-pulsatile tinnitus and high frequency sensorineural hearing loss. Less often, they may present with symptoms related to mass effect upon the middle cerebellar peduncle, lateral pons, and/or the cisternal trigeminal nerve. The presence of bilateral vestibular schwannomas is diagnostic of neurofibromatosis type II.

Vestibular schwannomas are typically difficult to identify on CT unless quite large. Expansion of the internal auditory canal may be present. On MR imaging, they are heterogeneous on T1- and T2-weighted images and enhance following contrast administration. When large (greater than 2 cm), they often show cystic degeneration. Approximately 5–10% of vestibular schwannomas may have a co-existent arachnoid cyst. Hemorrhage and calcification are rare, unless previ-

ously treated [17]. Foci of micro-hemorrhage, identified as susceptibility-related signal loss, is a highly specific finding in schwannomas as compared with meningiomas [18]. When evaluating a patient with a vestibular schwannoma, it is important to identify the full extent of the neoplasm including extension to the cochlear aperture and/or cerebello-pontine angle, and to describe the presence of mass effect on the middle cerebellar peduncle and brainstem. Approximately 60–75% of vestibular schwannomas involve the internal auditory canal and the cerebello-pontine angle.

The goal of management of vestibular schwannomas over the last decade has shifted from "complete resection" to hearing preservation. Treatment may include surgical resection or stereotactic radiosurgery. Clinical and radiologic observation is now common for small, stable tumors [19].

15.6.2 Cholesteatoma

Cholesteatoma is an expansile erosive mass lined by keratinizing stratified squamous epithelium. It may result from a congenital inclusion of squamous epithelium in the middle ear cavity (congenital cholesteatoma), or more commonly from abnormal migration of squamous epithelium into the middle ear cavity through a perforated tympanic membrane because of chronic infection/inflammation. Otoscopic examination typically reveals a pearly white mass behind the tympanic membrane. Erosive enzymes and osteoclast-stimulating agents within the epithelial debris cause bone destruction, the radiologic hallmark of this pathology. Acquired cholesteatomas most often occur in the setting of an underpneumatized mastoid, a perforation of the pars flaccida (Shrapnell's membrane), involve Prussak space, and erode the adjacent bone including the scutum and ossicles (the mallear head and incus body). The ossicles may be displaced medially. Cholesteatomas related to pars tensa perforations are less common. In these lesions, the sinus tympani, pyramidal eminence, and facial nerve recess may be involved, as well as the long process of the incus and the stapes suprastructure.

In the imaging evaluation of patients with a cholesteatoma, it is important to comment on the extent of middle ear cavity opacification. Specifically, it is important to note if there is involvement of the anterior epitympanic recess, round window niche, sinus tympani, and/or facial recess. The radiologist should comment on the integrity of adjacent bone including the roof of the epitympanum (the tegmen tympani), the lateral semicircular canal, and the facial nerve canal. It is also important to address relevant surgical anatomy, such as the presence of a high or dehiscent jugular bulb, or an anteriorly positioned sigmoid sinus plate. Non-echo planar diffusion-weighted MR imaging is valuable in distinguishing cholesteatomas (which typically have restricted diffusion) from inflammatory opacification in the middle ear cavity (which typically have facilitated diffusion). Frequently both are present, and DWI can distinguish the cholesteatoma from areas of inflammation [20, 21]. Inflammatory disease also typically enhances, contributing to the distinction of these entities.

15.6.3 Glomus Tumor

Glomus tympanicum is a paraganglioma that arises from glomus bodies along the course of Jacobson's nerve (the tympanic branch of CN IX) along the lateral aspect of the cochlea in the middle ear cavity. Glomus tympanicum is the most common primary tumor of the middle ear in adults and presents in middle age with a slight female predominance. The typical clinical presentation is pulsatile tinnitus. Patients may also have conductive hearing loss. On otoscopic examination, a fleshy vascular mass behind the tympanic membrane in the middle ear cavity is most often identified.

When imaging a patient with a suspected glomus tympanicum, the radiologist should first evaluate for and exclude other causes of pulsatile tinnitus. These include vascular anomalies such as an aberrant internal carotid artery, high riding dehiscent jugular bulb, jugular vein or sigmoid diverticulum (outpouching of the jugular bulb or sigmoid sinus, respectively, into adjacent pneumatized temporal bone), and large condylar or mastoid emissary veins that traverse air cells.

The classic imaging appearance is a demarcated mass along the cochlear promontory (Fig. 15.5)**.** These tumors are soft tissue in density on CT, and on MR imaging they are iso- to mildly hyperintense to CSF on T1-weighted imaging, mildly hyperintense on T2-weighted imaging, and enhance

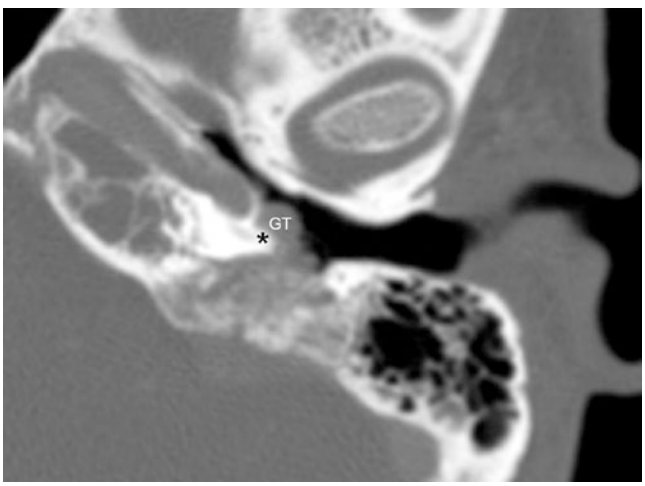

Fig. 15.5 Glomus tympanicum. Axial multi-detector CT image of the left temporal bone shows a soft tissue mass (GT) at the cochlear promontory (asterisk)

intensely following contrast administration [22]. DOTATATE Positron Emission Tomography (PET) has recently emerged as a valuable adjunct to CT and MR imaging for the evaluation of these lesions [23]. While these tumors are very vascular, the typical "salt and pepper" appearance seen in other glomus tumors/paragangliomas is frequently not seen in glomus tympanicum tumors due to their relatively small size. Once establishing the presence of a glomus tympanicum it is important to determine the extent of disease. These tumors are classified based on their spread from the cochlear promontory to the middle ear cavity/ossicles, inner ear structures, external auditory canal, carotid canal, and the mastoid air cells. The radiologist should specify if the tumor is confined to the middle ear cavity (glomus tumors tend to engulf rather than erode the ossicles), identify if there is fistulization to the inner ears structures due to bone erosion, and identify extension of tumor into adjacent structures.

When there is tumor in the jugular foramen, it is important to establish if the middle ear tumor is a projection of a larger glomus tumor arising in the jugular fossa—a glomus jugulare-tympanicum. Glomus jugulare paragangliomas arise from glomus bodies in the jugular foramen, either in the adventitia of the jugular bulb, the superior ganglion of cranial nerve CN X, or along Arnold or Jacobsen nerves (auricular branch of CN X and tympanic branch of CN IX, respectively). They frequently grow directly into the jugular vein (Fig. 15.6a, b).

15.6.4 Cholesterol Granuloma

Lucent, expansile lesions of the petrous apex (cholesterol granuloma, mucocele, epidermoid, meningocele) are common. They are frequently incidental lesions detected on head CTs performed for unrelated reasons. These lesions may be symptomatic when they produce mass effect on adjacent structures. The management of each petrous apex lesion is different, and the clinical history is often of limited use. Biopsy is often difficult to perform, and in certain instances are contraindicated as they may potentially harm the patient. Fortunately, a specific diagnosis can usually be made using a combination of CT and MR imaging [24, 25]. On CT, the pattern of bone expansion, remodeling, and/or erosion are important. On MR imaging, the signal intensity on T1, T2, T2 FLAIR, DWI, and enhanced T1 weighting are often diagnostic-cholesterol granulomas are typically hyperintense on unenhanced T1-weighted imaging and epidermoids classically have restricted diffusion [24, 25]. It is important to describe the size, the location of the lesion, and its relationship to adjacent critical structures, including the petrous internal carotid artery and the internal auditory canal.

Cholesterol granulomas typically arise in a pneumatized space, most often the petrous apex of the temporal bone. It is thought that these develop due to recurrent microhemorrhages at the capillary level, which may result from negative pressures in petrous air cells. The blood incites a mucosal reaction, giant cells, and cholesterol crystal deposition leading to recurrent hemorrhage. This cycle results in petrous apex expansion which can cause cranial nerve symptoms (CNs V and VIII) and tinnitus. The resulting appearance is an expansile, lytic, circumscribed mass centered in the petrous apex, that is often unilocular (Fig. 15.7a). On MR imaging, cholesterol granulomas are characteristically hyperintense on T1-weighted images related to methemoglobin (Fig. 15.7b) though they may be heterogeneous on all pulse sequences due to blood products of varying ages.

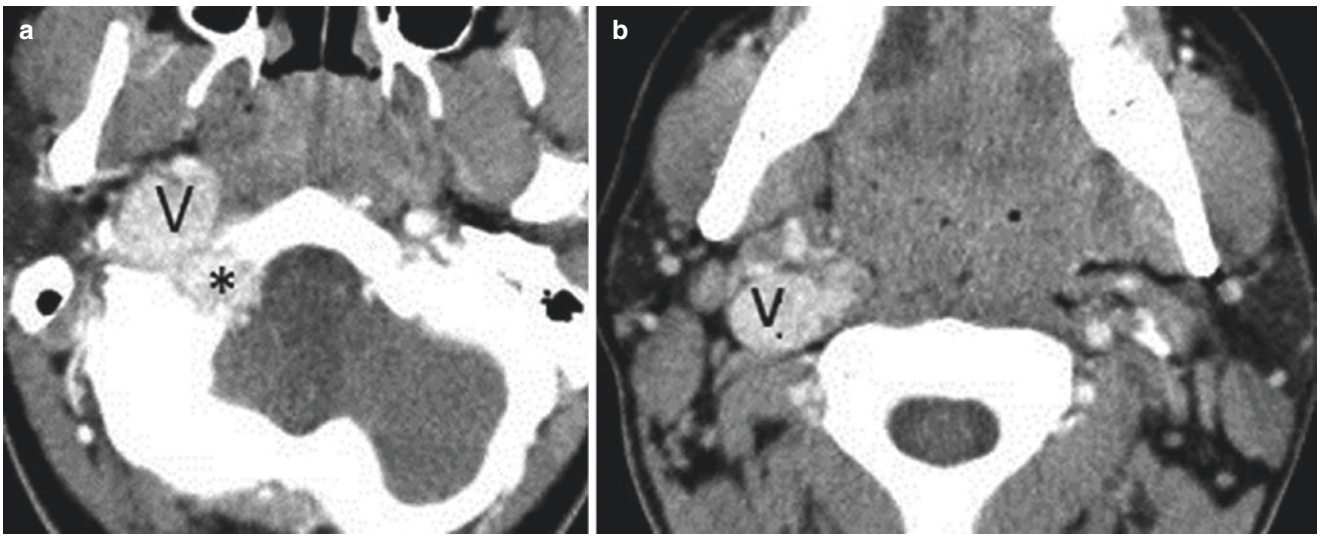

Fig. 15.6 (**a**, **b**) Glomus jugulare. Axial enhanced CT images show a vascular avidly enhancing mass in the jugular foramen (*), with direct inferior growth into the internal jugular vein (V)

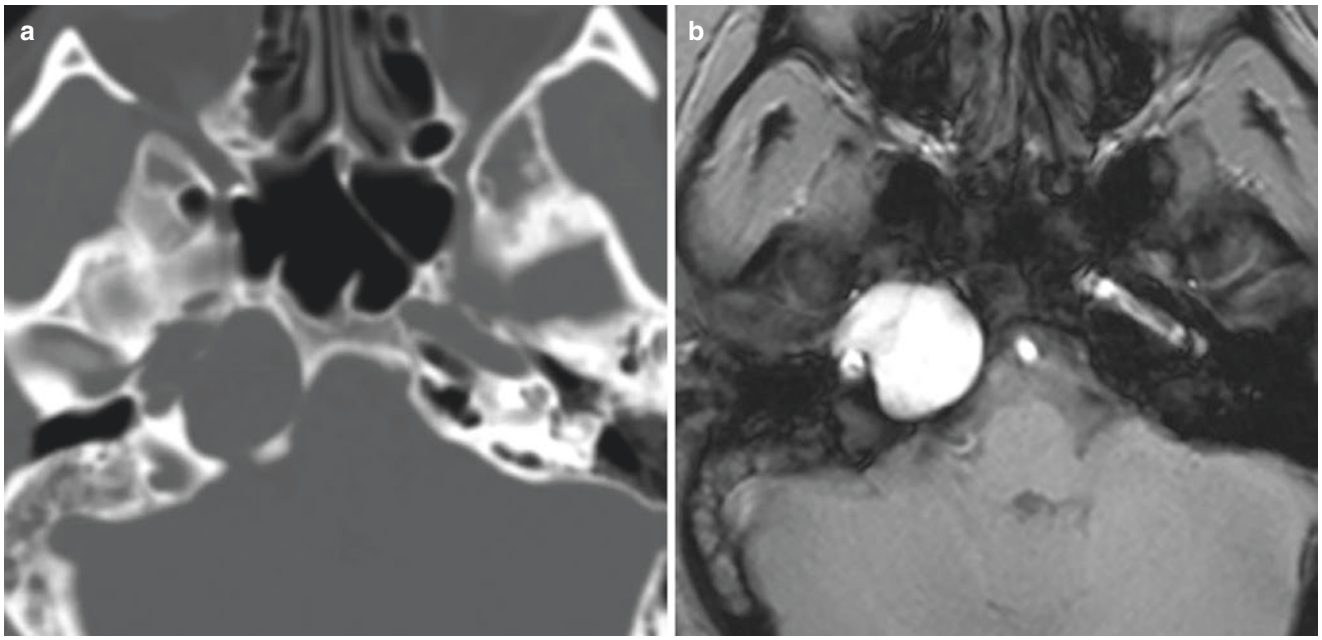

Fig. 15.7 (**a**, **b**) Cholesterol granuloma. (**a**) Axial CT image in bone window shows a unilocular, expansile mass of the right petrous apex. (**b**) Axial unenhanced T1-weighted gradient image shows the characteristic hyperintensity of these lesions related to blood products. The right mastoid air cells are opacified

15.7 Conclusion

The imaging workup for tinnitus and hearing loss in adults follows otoscopic exam and audiometry testing. Computed tomography and MR imaging have different and often complimentary roles in the evaluation of tinnitus and hearing loss depending on the clinical scenario and the suspected underlying cause. Imaging can often identify the cause and evaluate the extent of disease for surgical planning.

Take-Home Messages

- The radiologist should be familiar with a few key temporal bone anatomical structures and levels on axial and coronal imaging.
- The imaging approach and differential for hearing loss and tinnitus can be based on whether a mass is present or absent.
- MR and CT are complementary modalities. The choice of imaging modality depends on the most likely clinical diagnosis following history and otoscopic examination.

References

1. Langguth B, Kreuzer PM, Kleinjung T, De Ridder D. Tinnitus: causes and clinical management. Lancet Neurol. 2013;12(9):920–30.
2. Deafness and hearing loss fact sheet. World Health Organization. 27 Feb 2023. Retrieved 25 Aug 2023.
3. Little SC, Kesser BW. Radiographic classification of temporal bone fractures: clinical predictability using a new system. Arch Otolaryngol Head Neck Surg. 2006;132(12):1300–4.
4. Benson JC, Carlson ML, Lane JI. MRI of the internal auditory canal, labyrinth, and middle ear: how we do it. Radiology. 2020;297(2):252–65.
5. El-Badry MM, Osman NM, Mohamed HM, Rafaat FM. Evaluation of the radiological criteria to diagnose large vestibular aqueduct syndrome. Int J Pediatr Otorhinolaryngol. 2016;81:84–91.
6. van Egmond SL, Stegeman I, Grolman W, Aarts MCJ. A systematic review of non-echo planar diffusion-weighted magnetic resonance imaging for detection of primary and postoperative cholesteatoma. Otolaryngol Head Neck Surg. 2016;154(2):233–40.
7. Lee TC, Aviv RI, Chen JM, Nedzelski JM, Fox AJ, Symons SP. CT grading of otosclerosis. AJNR Am J Neuroradiol. 2009;30(7):1435–9.
8. Marshall AH, Fanning N, Symons S, et al. Cochlear implantation in cochlear otosclerosis. Laryngoscope. 2005;115:1728–33.
9. Hartnick CJ, Kim HY, Chute PM, Parisier SC. Preventing labyrinthitis ossificans. Arch Otolaryngol Neck Surg. 2001;127(2):180.
10. Juliano AF, Ginat DT, Moonis G. Imaging review of the temporal bone: part I. Anatomy and inflammatory and neoplastic processes. Radiology. 2013;269(1):17–33.

11. Berning AW, Arani K, Branstetter BF. Prevalence of superior semicircular canal dehiscence on high-resolution CT imaging in patients without vestibular or auditory abnormalities. AJNR Am J Neuroradiol. 2019;40(4):709–12.
12. Wieczorek SS, Anderson ME, Harris DA, Mikulec AA. Enlarged vestibular aqueduct syndrome mimicking otosclerosis in adults. Am J Otolaryngol. 2013;34(6):619–25.
13. Mori T, Westerberg BD, Atashband S, Kozak FK. Natural history of hearing loss in children with enlarged vestibular aqueduct syndrome. J Otolaryngol Head Neck Surg. 2008;37(1):112–8.
14. Naganawa S, Ito T, Iwayama E, et al. MR imaging of the cochlear modiolus: area measurement in healthy subjects and in patients with a large endolymphatic duct and sac. Radiology. 1999;213(3):819–23.
15. Madden C, Halsted M, Meinzen-Derr J, et al. The influence of mutations in the SLC26A4 gene on the temporal bone in a population with enlarged vestibular aqueduct [published correction appears in Arch Otolaryngol Head Neck Surg. 2007 Jun;133(6):607]. Arch Otolaryngol Head Neck Surg. 2007;133(2):162–8.
16. Saliba I, Gingras-Charland M-E, St-Cyr K, Décarie J-C. Coronal CT scan measurements and hearing evolution in enlarged vestibular aqueduct syndrome. Int J Pediatr Otorhinolaryngol. 2012;76(4):492–9.
17. Shahbazi T, Sabahi M, Arjipour M, Adada B, Borghei-Razavi H. Hemorrhagic vestibular schwannoma: case report and literature review of incidence and risk factors. Cureus. 2020;12(9):e10183.
18. Thamburaj K, Radhakrishnan VV, Thomas B, Nair S, Menon G. Intratumoral microhemorrhages on T2*-weighted gradient-echo imaging helps differentiate vestibular schwannoma from meningioma. AJNR Am J Neuroradiol. 2008;29(3):552–7.
19. Lin EP, Crane BT. The management and imaging of vestibular schwannomas. Am J Neuroradiol. 2017;38(11):2034–43.
20. Schwartz KM, Lane JI, Bolster BD, Neff BA. The utility of diffusion-weighted imaging for cholesteatoma evaluation. Am J Neuroradiol. 2011;32(3):430–6.
21. Dremmen MH, Hofman PA, Hof JR, Stokroos RJ, Postma AA. The diagnostic accuracy of non-echo-planar diffusion-weighted imaging in the detection of residual and/or recurrent cholesteatoma of the temporal bone. AJNR Am J Neuroradiol. 2012;33(3):439–44.
22. Alaani A, Chavda SV, Irving RM. The crucial role of imaging in determining the approach to glomus tympanicum tumours. Eur Arch Otorhinolaryngol. 2009;266(6):827–31.
23. Rini JN, Keir G, Caravella C, Goenka A, Franceschi AM. Somatostatin receptor-PET/CT/MRI of head and neck neuroendocrine tumors. AJNR Am J Neuroradiol. 2023;44(8):959–66.
24. Schmalfuss IM. Petrous apex. Neuroimaging Clin N Am. 2009;19(3):367–91.
25. Chapman PR, Shah R, Cure JK, Bag AK. Petrous apex lesions: pictorial review. Am J Roentgenol. 2011;196(3):WS26–37.